Trapping effect and high-lying single-particle modes

Ch. Stoyanov
Institute for Nuclear Research and Nuclear Energy, Boul. Tzarigradsko Chaussee 72, 1784 Sofia, Bulgaria

I. Rotter
Max-Planck-Institut für Physik komplexer Systeme, D-01187 Dresden, Germany
and Technische Universität Dresden, Institut für Theoretische Physik, D-01062 Dresden, Germany

N. Van Giai
Division de Physique Théorique, Institut de Physique Nucléaire, F-91406 Orsay Cedex, France
(Received 16 February 1999; published 19 November 1999)

The phenomenon of trapping of states is studied in the case of high-lying states with large angular momentum in the odd-*A* nucleus ^{209}Pb. The interaction of the single-particle mode with more complex states is calculated in the framework of the quasiparticle-phonon model while the coupling to the continuum is included by means of the projection operator method. The results obtained show a reduction of the spreading of the single-particle strength under the influence of the coupling to the continuum: the strength is concentrated on a few collective states while the remaining states are decoupled from the continuum (trapped). The results are compared with the case where continuum coupling is switched off. The influence of the continuum on the nuclear structure should be visible in nucleon transfer reactions. [S0556-2813(99)01812-9]

PACS number(s): 21.10.Pc, 21.10.Jx, 21.60.−n, 25.55.Hp

I. INTRODUCTION

In the last years, the microscopic structure of nuclear excitations embedded in the continuum has received great interest. As an example, nucleon transfer reactions at intermediate energies reveal resonancelike structures which arise from the excitation of high angular momentum states lying above the particle emission threshold [1–5]. These structures originate from the coupling of a single-particle mode to more complex states [1,6,7]. The coupling can directly be measured through the width of the single-particle state.

The highly excited resonancelike structures arise from states which are embedded in the continuum of decay channels. The properties of such states were recently discussed in different fields of physics: in nuclear physics [8–11], atomic physics [12], quantum chemistry [13], as well as in more formal systems such as quantum billiards [14]. Common to all these studies is the phenomenon of trapping of states appearing at high level density. It consists in the following.

Generally, the states embedded in the continuum of decay channels can interact not only directly but also via the continuum. The interaction between these states is described by $V^{\rm eff}=V_{QQ}+W_{QPQ}$ where V_{QQ} is the direct (internal) interaction and W_{QPQ} the (external) interaction of the states via the continuum. The matrix elements of W_{QPQ} are complex [8,13]. When the states start to overlap, i.e., when $\overline{\Gamma}\approx\overline{D}$, where $\overline{\Gamma}$ is the average width and $\overline{D}$ is the average distance of the states, a redistribution takes place in the system: some states become trapped, i.e., long lived, while others align with the decay channels and become short lived. As a result, the width's distribution is broadened [10] as compared to the χ^2 distribution characteristic of the random matrix theory. The alignment of some states with the decay channels and the trapping of the remaining states is achieved by the interplay between the two parts of $V^{\rm eff}$.

In Ref. [9], the collectivity of the short-lived states originating from their alignment with the decay channels is called external collectivity. It occurs additionally to the well-known collectivity of intrinsic nature considered in the damping process of single-particle modes. At high level density, the external and internal collectivity interfere and influence significantly the distribution of the simple modes as well as their widths and positions in energy [9]. This study is performed in the framework of a schematical model.

The goal of the present paper is to study the influence of the coupling to the continuum on the properties of the single-particle states in a realistic case. For this purpose, calculations are performed for the $l_{19/2}$ neutron state in ^{209}Pb using the method proposed in Refs. [6,15]. The interaction of the single-particle mode with more complex states, i.e., the spreading effect, is calculated in the framework of the quasiparticle-phonon model (QPM) [7,16] while the coupling to the continuum is included by means of the projection operator method [17].

The paper is organized as follows. In Sec. II we sketch the theoretical approach to treat the direct nucleon decay of high angular momentum states of single-particle type. In Sec. III the results obtained for the $l_{19/2}$ neutron state in ^{209}Pb are presented and analyzed from the point of view of the trapping phenomenon. Finally, in Sec. IV the results are discussed and some conclusions are drawn.

II. THEORY

A. Formalism

A convenient approach for dealing with problems involving single-particle continua is the projection operator method. The general formalism, introduced for heavy nuclei by Yoshida and Adachi [17], has been applied to studies of

particle decays of giant resonances [18,19,21] as well as of high-lying states in odd nuclei [6,15,20]. We recall briefly the main steps of the method used in the present work. Further details can be found in Ref. [15].

The Hamiltonian of the $A+1$ system can be written as

$$H=\sum_{i=0}^{A} h_i+\frac{1}{2}\sum_{i,j=0}^{A} V_{ij}$$
$$=h+H_{core}+\sum_{i=1}^{A} V_{0i}. \quad (1)$$

In the first line, h_i describes the motion of a particle in an average potential U created by the other particles and V_{ij} is the residual interaction between particles. In the second line, we have separated out the Hamiltonian H_{core} of the A-particle core.

A set of discrete orthonormal single-particle states $\{\phi_\alpha,\epsilon_\alpha\}$ is constructed by diagonalizing h on a harmonic oscillator basis. Here, α stands for the quantum numbers $(nljm)$ defining a single-particle state. We denote by $a_\alpha^\dagger, a_\alpha$ the creation and annihilation operators of state α. The space spanned by the set $\{\phi_\alpha\}$ is called the q space and the corresponding projection operator is q. The complementary p space with projection operator $p\equiv 1-q$ and creation and annihilation operators $a_\epsilon^\dagger, a_\epsilon$ for particles in the scattering states ϵ can be built by solving the Schrödinger equation with the projected Hamiltonian php [17].

In the framework of QPM the Hamiltonian H_{core} [7] is treated in the random-phase approximation (RPA) in a discrete space, i.e., the particle-hole configurations of RPA are built only with q-space states. We denote by E_ν and $O_\nu^\dagger$ the energies and creation operators of these RPA states which describe core excitations. If $|0\rangle$ represents the RPA ground state of the core, the properties of the $(A+1)$ nucleus can be described in terms of the one-particle states $a_\alpha^\dagger|0\rangle$ and one-particle-plus-phonon states $[a_\beta^\dagger\otimes O_\nu^\dagger]|0\rangle$. We can write

$$|d_i\rangle\equiv d_i^\dagger|0\rangle=\left(\sum_\alpha C_\alpha^{(i)}a_\alpha^\dagger+\sum_{\beta,\nu} D_{\beta,\nu}^{(i)}[a_\beta^\dagger\otimes O_\nu^\dagger]\right)|0\rangle. \quad (2)$$

The space spanned by the (real) state vectors $|d_i\rangle$ is called Q space with projection operator Q. The amplitudes $C_\alpha^{(i)}$ and $D_{\beta,\nu}^{(i)}$, and the energies ω_i of $|d_i\rangle$ are determined by diagonalizing H in the RPA, i.e., one solves

$$[QHQ,d_i^\dagger]=\omega_i d_i^\dagger \quad (3)$$

within the approximation of commutator linearization. The distribution of $|C^{(i)}|^2$ represents the strength function from which one can deduce the spectroscopic factors [1].

The P space complementary to the Q space consists of all states which are linear combinations of the following one-particle and one-particle-plus-phonon configurations:

$$|\epsilon\rangle\equiv a_\epsilon^\dagger|0\rangle, \quad |\epsilon,\nu\rangle\equiv[a_\epsilon^\dagger\otimes O_\nu^\dagger]|0\rangle. \quad (4)$$

This definition of P space neglects continuum effects on the phonons $O_\nu^\dagger$. This is a reasonable assumption since only low-lying phonons turn out to be important. Denoting the projector on P space by P, the properties of the $A+1$ system including continuum effects are determined by the following effective Hamiltonian, which is complex and energy-dependent:

$$\mathcal{H}(E)=QHQ+QHP\frac{1}{E^{(+)}-PHP}PHQ\equiv H_{QQ}+W(E), \quad (5)$$

where E is the energy of the system. For each value of E one has to find the set of complex eigenfunctions and eigenenergies of $\mathcal{H}$:

$$|\mathcal{D}_i\rangle\equiv\mathcal{D}_i^\dagger|0\rangle=\left(\sum_\alpha \tilde{\mathcal{C}}_\alpha^{(i)}a_\alpha^\dagger+\sum_{\beta,\nu}\tilde{\mathcal{D}}_{\beta,\nu}^{(i)}[a_\beta^\dagger\otimes O_\nu^\dagger]\right)|0\rangle, \quad (6)$$

satisfying

$$[\mathcal{H}(E),\mathcal{D}_i^\dagger]=\Omega_i\mathcal{D}_i^\dagger, \quad (7)$$

again within the approximation of commutator linearization. The $\Omega_i=\overline{\omega_i}-i\Gamma_i^\uparrow/2$ are the complex eigenvalues of $\mathcal{H}$.

B. Model for the structure of the states

We have used the QPM of Soloviev and co-workers [7,16] to study the trapping effect on the high-lying single-particle mode. This model has often been used in spectroscopic studies of medium and heavy nuclei where it gives distributions of spectroscopic strengths in satisfactory agreement with experimental data extracted from transfer reactions [1]. The neutron decay of high angular momentum states in the nuclei ^{209}Pb and ^{91}Zr has been studied in the framework of QPM in Refs. [15] and [20]. It is therefore interesting to test the predictions of the model in the context of a more detailed description of the influence of the continuum on the properties of highly excited states.

The advantage of the QPM is that its two-body residual interaction is chosen to be of multipole-multipole separable form. Therefore the task of determining the eigenvalues and eigenvectors of the Hamiltonian is simplified. This enables one to work with configuration spaces of large dimensions without facing the cumbersome problem of diagonalizing large matrices.

The mean potentials entering the single-particle Hamiltonians h_i are chosen to be Woods-Saxon potentials. The guidelines for determining their parameters are the values given in Refs. [22] and [23]. The corresponding single-particle spectra can be found in Ref. [1]. These parameters are readjusted in such a way that, once the coupling to phonons is included, the ground state of an odd nucleus is located at the experimental position with respect to the neutron separation threshold.

The residual particle-hole interaction of Eq. (1) is taken of separable form in coordinate space with effective interaction strengths considered as adjustable parameters. For the radial interaction form factor we have used $f(r)=dU/dr$ where $U(r)$ is the central part of the Woods-Saxon potential. For each excitation mode of the even-even core corresponding to given angular momentum, parity, and isospin, the interaction

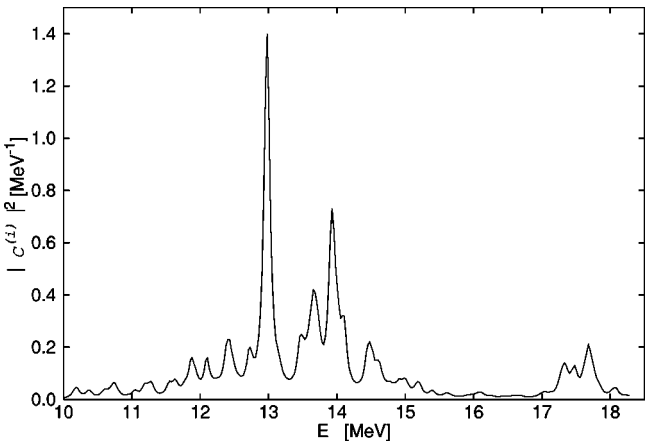

FIG. 1. Strength function of the $l_{19/2}$ neutron state in ^{209}Pb as a function of the excitation energy.

strength is found by requiring that the energy of the lowest collective state calculated in RPA coincides with the experimental energy. These interaction strengths are also used for the quasiparticle-phonon coupling. These low-lying phonons of the core are the physical channels into which the initial state in the excited odd-A nucleus can decay by semi-direct particle emission.

The quasiparticle-phonon interaction introduced in the model can mix states which differ by one phonon. The simple wave function (2) describes in detail the distribution of the single-particle component while the distribution of particle-plus-phonon components could be more affected by including particle-plus-two-phonons components [1].

III. RESULTS

A. Demonstration of the trapping effect

Using the method presented in the foregoing section, we have calculated the influence of the continuum on the $l_{19/2}$ neutron state in ^{209}Pb. The chosen state is quasibound in Woods-Saxon potential and its energy, $E_{WS}(l_{19/2})=8.46$ MeV, is several MeV higher than those of the $k_{17/2}$ and $j_{13/2}$ states of ^{209}Pb studied in Ref. [15] ($E_{WS}(k_{17/2})=4.88$ MeV and $E_{WS}(j_{13/2})=5.50$ MeV). Therefore it should be more sensitive to the influence of the continuum than the other two states. In the present calculations we have used a slightly larger radius for the neutron potential than in Ref. [15] in order to enhance the effect of the $l_{19/2}$ continuum.

Let us first discuss the distribution of the single-particle strength in the discrete Q subspace. This space corresponds to the so-called internal space, where the interaction between the single-particle state and particle-plus-phonon ones spreads the single-particle strength over the eigenvectors of QHQ. According to Eq. (3) the Hamiltonian H is diagonalized in the Q space and the energies ω_i and amplitudes $C^{(i)}, D^{(i)}$ of the states are found.

At high excitation energy, the level density is large and it is convenient to calculate the strength function of the single-particle state [1,16] using an averaging Lorentzian function of width $\Delta=0.1$ MeV. The strength function of the $l_{19/2}$ state is shown in Fig. 1. It is concentrated at an excitation energy between 12 and 15 MeV. There is, however, a high energy tail between 17 and 18 MeV where 11% of the strength appear. The calculated characteristics of the strength function in the domain of the main peak (11–15.5 MeV) are as follows: centroid $\bar{E}=13.3$ MeV, variance $\sigma=0.82$ MeV, single-particle strength $\Sigma|C^{(i)}|^2=74\%$.

To study the influence of the continuum on the distribution of the single-particle strength, the term $W(E)$ in Eq. (5) is replaced by the term

$$W'(E)=\alpha W(E), \tag{8}$$

where α is a parameter. This allows us to study the properties of the system as a function of the coupling strength of the single-particle state to the continuum. The value $\alpha=1$ corresponds to the realistic coupling strength of the single-particle state to the continuum and to the realistic interaction between particle and phonon as used in Ref. [15]. To be more illustrative we have varied α only for the imaginary part of $W(E)$ and fixed it to $\alpha=1$ for the real part of Eq. (8). The variation of the real part of $W(E)$ with α will be discussed below.

We first examine the simple case where the decay channels related to excited states of the core are neglected. This amounts to keep in the P space the components $|\epsilon\rangle\equiv a_\epsilon^\dagger|0\rangle$ only [see Eq. (4)]. The eigenvalues of the effective Hamiltonian (5) calculated at the excitation energy $E=13.3$ MeV of the system for different values of the parameter α are shown in Fig. 2. The contribution of the single-particle amplitude in the norm of the wave function (6) is denoted by $|\tilde{\mathcal{C}}^{(i)}|^2$. Its distribution is given in Fig. 3.

Figure 2(a) corresponds to $\alpha=1$. Because of the strong interaction of particle and particle-plus-phonon states in the discrete space, the particle strength is distributed in a large energy domain and many eigenvalues have a large imaginary part. Its distribution is correlated with that of the $|\tilde{\mathcal{C}}^{(i)}|^2$ [Fig. 3(a)]. The maximum of the imaginary part of the eigenvalue is at the same energy as the maximum of the amplitude. In comparison with Fig. 1, there is a downward shift (from 13 to 12.70 MeV) of the maximum which is caused by the interaction with the continuum.

The distribution of the eigenvalues and of the $|\tilde{\mathcal{C}}^{(i)}|^2$ for $\alpha=3$ is shown in Figs. 2(b) and 3(b), respectively. It can be seen that enlarging of α leads to a concentration of the imaginary part of the eigenvalues predominantly on a few states. This result is caused by the trapping effect, i.e., by the interference of the states in the complex energy plane which causes a redistribution of the imaginary parts of the eigenvalues. As a result there are, at large α, many narrow states and one broad state. The distribution of $|\tilde{\mathcal{C}}^{(i)}|^2$ shows a similar behavior. The corresponding values of $|\tilde{\mathcal{C}}^{(i)}|^2$ are 55% on one state at $\alpha=3$ [Fig. 3(b)], while the maximum value in Fig. 3(a) is only 19%. Further increasing of α results in still more concentration of $|\tilde{\mathcal{C}}^{(i)}|^2$. For example, the value $\alpha=10$ leads to a concentration of 85% of $|\tilde{\mathcal{C}}^{(i)}|^2$ on one state.

Let us now consider the more complex system having several open decay channels. The physical channels of the

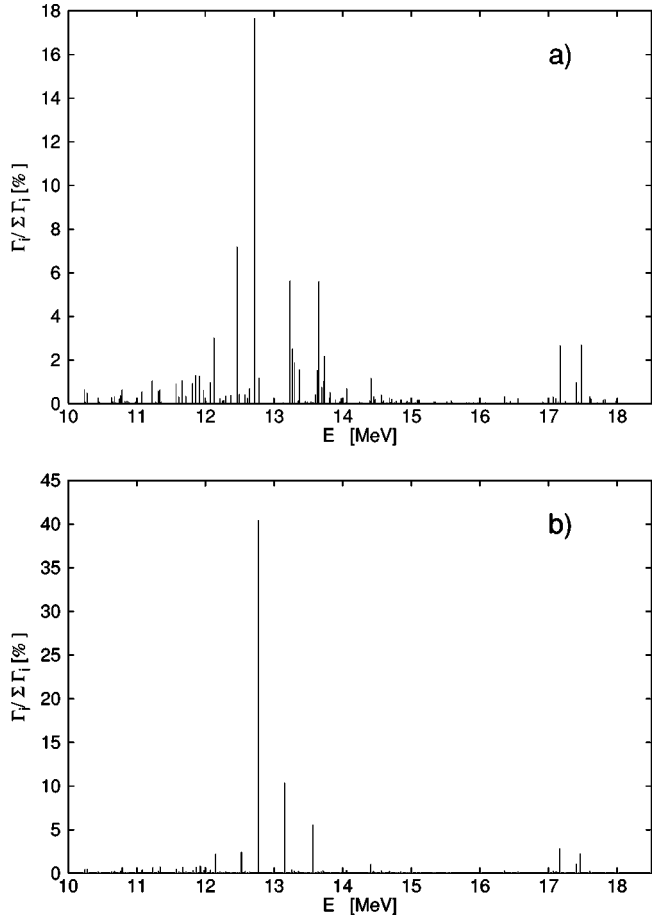

FIG. 2. Eigenvalues of the effective Hamiltonian (5) calculated at the excitation energy of the system $E=13.3$ MeV. Only the ground state channel is included. The imaginary part is normalized to the sum of all imaginary parts. The calculation is performed for (a) $\alpha=1$, (b) $\alpha=3$.

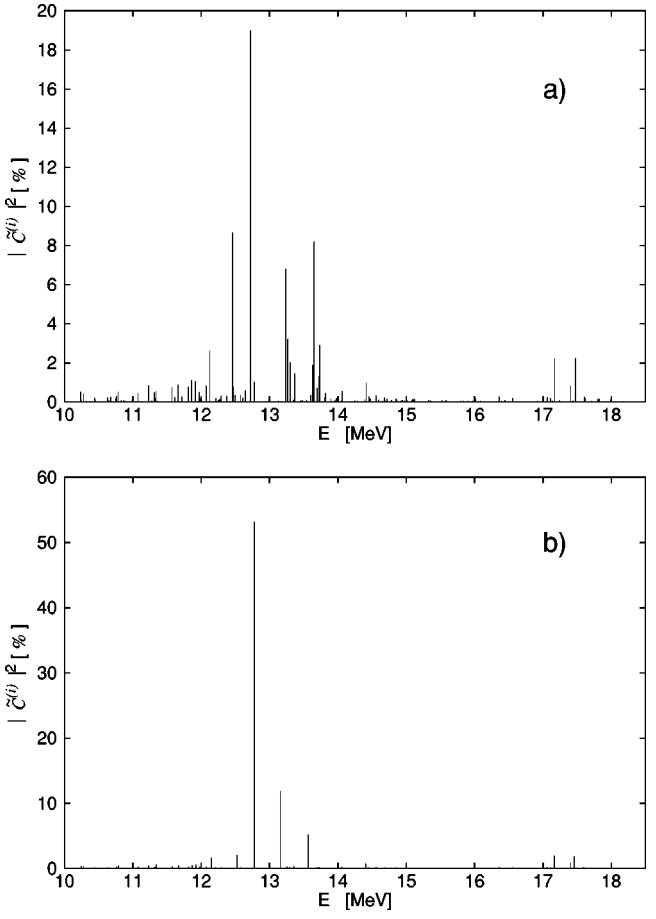

FIG. 3. Distribution of the single-particle strength $|\tilde{C}^{(i)}|^2$ calculated at the excitation energy of the system $E=13.3$ MeV. Only the ground state channel is included. The calculation is performed for (a) $\alpha=1$, (b) $\alpha=3$.

system correspond to the ground state and the low-lying phonon excitations of the even-even core. In the present calculations these are the first $\nu=2^+,3^-,4^+,5^-,6^+,7^-$, and 8^+ excited states in ^{208}Pb. The P space now consists of all configurations shown in Eq. (4) built with these low-lying phonons. The rest of the phonons of course contributes to the Q space. The eigenvalues of the effective Hamiltonian in the case when the excited channels are taken into account are presented in Fig. 4. The calculation is performed at the same excitation energy of the system as in Figs. 2 and 3 ($E=13.3$ MeV). The large difference between the imaginary parts of the eigenvalues plotted in Figs. 2 and 4 arises from the influence of the new open channels. For $\alpha=1$ there are many eigenvalues with a large imaginary part [Fig. 4(a)]. For larger value of α the number of such eigenvalues is reduced [Fig. 4(b)].

The structure of the eigenvectors is complex and depends on the value of α. The contribution of the single-particle component in the norm of the wave function (6) is given in Table I. For $\alpha=1$ large fractions of the single-particle component are shared between several states. The contribution of the excited channels in the structure is large. For $\alpha=3$ the number of eigenvectors containing a large part of the single-particle component is reduced. The same effect can be seen in Fig. 5 where the distribution of $|\tilde{C}^{(i)}|^2$ is shown. There is a strong shift in energy due to continuum coupling. Comparing Figs. 4(a) and 5(a) we can see that the correlation between the distributions of widths (obtained from the eigenvalues) and of $|\tilde{C}^{(i)}|^2$ do no longer exist. This is contrarily to the special case when only the ground state channel is included, see Figs. 2(a) and 3(a).

The components connected with the open excited channels have, as a function of α, the same behavior as the single-particle component (ground state channel). Their concentration in a few eigenvectors increases with increasing α. The reason for the redistribution of the strength is, in any case, the coupling of the states via the continuum. If the coupling strength increases, the interferences in the complex energy plane lead to the coexistence of a few short-lived states with a large amount of long-lived ones.

It should be noted, however, that the fragmentation of particle-plus-phonon components is limited in our calculations because of the simplicity of the wave function (6). The extension of the configuration space by including particle-plus-two-phonons components will influence the distribution of particle-plus-phonon components [1].

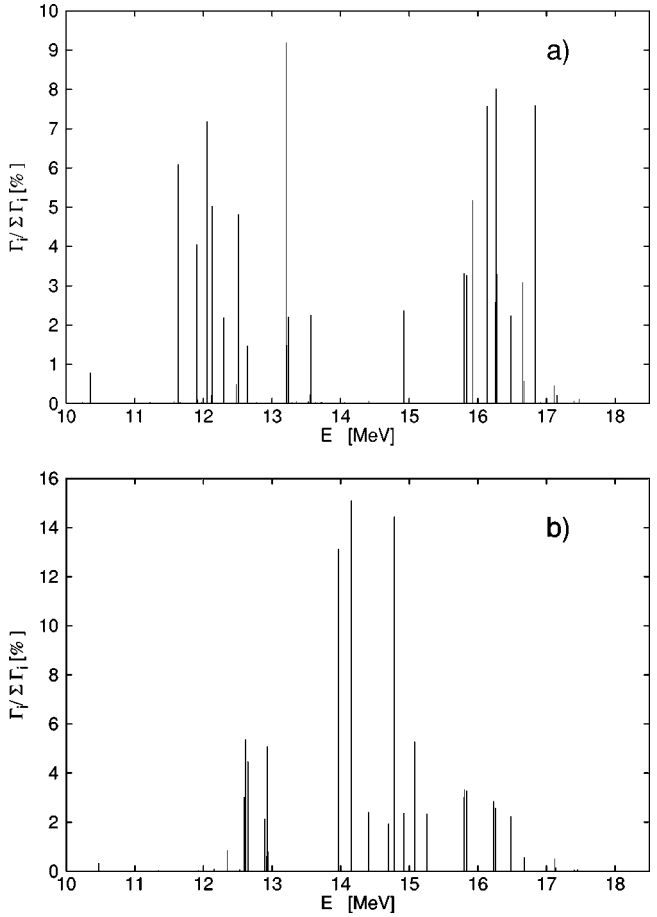

FIG. 4. Eigenvalues of the effective Hamiltonian (5) calculated at the excitation energy of the system $E=13.3$ MeV. The ground state and excited state channels are included. The imaginary part is normalized to the sum of all imaginary parts. The calculation is performed for (a) $\alpha=1$, (b) $\alpha=3$. The corresponding sum of the widths is $\Sigma\Gamma_i=23.46$ MeV at $\alpha=1$, and $\Sigma\Gamma_i=70.40$ MeV at $\alpha=3$.

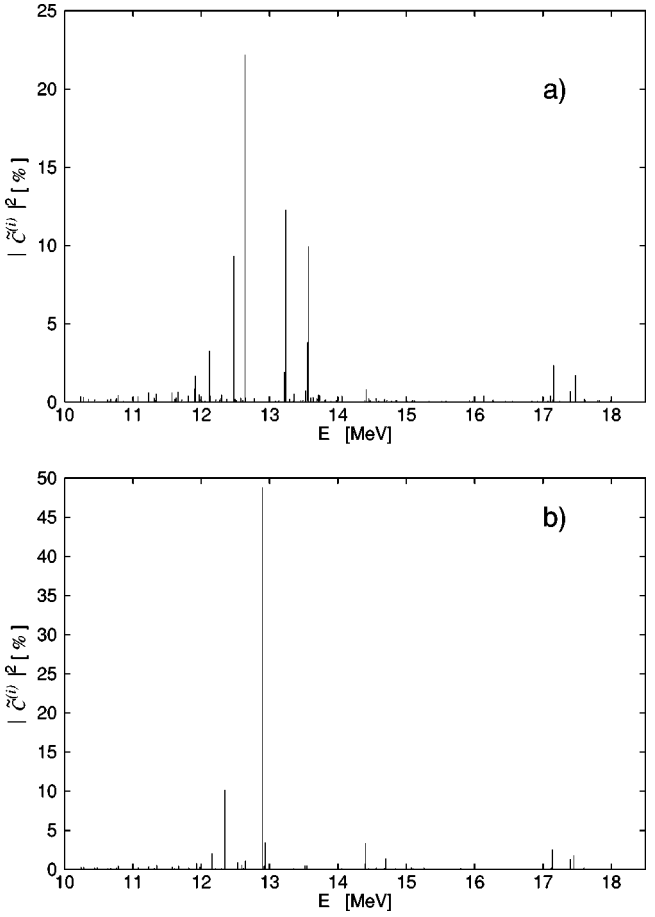

FIG. 5. Distribution of the single-particle strength $|\tilde{C}^{(i)}|^2$ calculated at the excitation energy of the system $E=13.3$ MeV. The ground state and excited state channels are included. The calculation is performed for (a) $\alpha=1$, (b) $\alpha=3$.

In the calculations shown in Figs. 2–5, we did not take into account the variation of the real part of $W(E)$ with α [Eq. (5)] and its influence on the spectrum. Its main effect is an energy shift of those eigenstates whose widths are large [8]. The influence of the real part of $W(E)$ on the distribution of single-particle amplitudes $|\tilde{C}^{(i)}|^2$ for $\alpha=3$ is as follows. The shape of the distribution is similar to that shown in Fig. 5(b) but the position of the main peak is somewhat shifted: The main state contains 59% of the single-particle amplitude and its energy is 11.80 MeV what is to compare with 49% and 12.89 MeV [Fig. 5(b)]. These results allow to conclude that the variation of the real part of $W(E)$ does not change

TABLE I. Selected eigenvalues (E, $\Gamma/2$), and structure of the corresponding eigenvectors showing the percentage of ground state and excited state channels. Only the states having largest spectroscopic factors are shown.

	E (MeV)	$\Gamma/2$ (MeV)	Structure
$\alpha=1$			
	12.48	0.06	9.3% $l_{19/2}$
	12.63	0.17	22% $l_{19/2}$+29% $[3_1^-\otimes i_{13/2}]$
	13.24	0.26	12% $l_{19/2}$+43% $[3_1^-\otimes i_{13/2}]$+14% $[5_1^-\otimes i_{13/2}]$
	13.57	0.26	10% $l_{19/2}$+64% $[5_1^-\otimes i_{13/2}]$
$\alpha=3$			
	12.35	0.29	10% $l_{19/2}$+65% $[3_1^-\otimes i_{13/2}]$
	12.89	0.75	49% $l_{19/2}$+16% $[3_1^-\otimes i_{13/2}]$

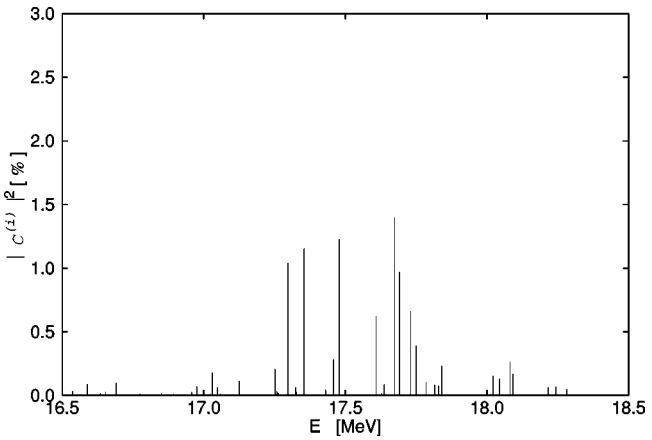

FIG. 6. Distribution of the high-energy tail of the single-particle strength $|C^{(i)}|^2$ in the discrete Q space.

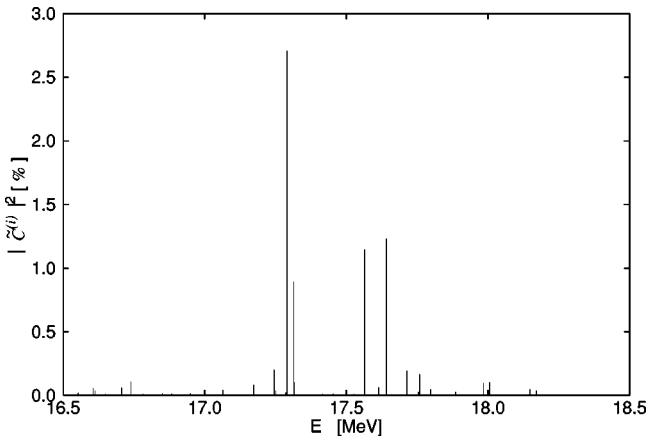

FIG. 7. Distribution of the high-energy tail of the single-particle strength $|\tilde{\mathcal{C}}^{(i)}|^2$ including continuum coupling. The calculation is performed at the excitation energy of the system $E=17$ MeV.

the conclusions about the trapping effect illustrated in Figs. 4(a), 4(b), 5(a), and 5(b).

B. Trapping effect and nucleon transfer

The knowledge of the single-particle strength distribution is important for the correct description of the nucleon transfer process. In the foregoing section we have shown that it may be influenced strongly by the coupling to the continuum. At low excitation energy, the single-particle state is only weakly affected by the continuum. In the case of the $l_{19/2}$ neutron state at excitation energy 13 MeV, we used therefore a large (nonrealistic) value of the parameter α in order to demonstrate the trapping effect. At higher excitation energy the influence of the continuum on the single-particle state is larger. In this case, a large redistribution of the single-particle strength could be expected even at the value of the parameter $\alpha=1$. For the $l_{19/2}$ neutron state, the domain strongly affected by the continuum at realistic coupling strength is expected therefore to be the high-energy tail of the strength function (Fig. 1). To study this domain in detail, we have diagonalized the effective Hamiltonian (5) at the excitation energy $E=17$ MeV of the system. The calculation is performed for $\alpha=1$, i.e., for the realistic coupling strength of the single-particle state to the continuum. The P space includes the states of Eq. (4).

First, we examine the single-particle strength distributions calculated in Q space only (no continuum coupling). The results are shown in Fig. 6. For several states the value of $|C^{(i)}|^2$ is around 1%. The characteristics of the distribution in the energy interval 16.5–18.5 MeV are as follows: centroid $\overline{E}=17.54$ MeV, variance $\sigma=0.30$ MeV and total single-particle strength $\Sigma|C^{(i)}|^2=10.48\%$. Next, the single-particle strength distribution calculated in the full $(P+Q)$ space (continuum coupling included) is shown in Fig. 7. The characteristics of the distributions in the same energy domain 16.5–18.5 MeV are: centroid $\overline{E}=17.42$ MeV, variance $\sigma=0.26$ MeV, total single-particle strength $\Sigma|\tilde{\mathcal{C}}^{(i)}|^2=8.06\%$.

The comparison of Figs. 6 and 7 shows above all that the strength is shared between a smaller number of states when the continuum coupling is included. The maximum value of $|\tilde{\mathcal{C}}^{(i)}|^2$ becomes about two times larger.

The redistribution of the single-particle strength could be tested via one-nucleon transfer reactions. The direct nucleon transfer followed by a semidirect neutron emission from a highly excited state is studied in Ref. [15]. Usually, the scattering amplitude is described in distorted wave Born approximation (DWBA) and therefore the most important ingredient is the nucleon-transfer matrix element. This matrix element is proportional to the single-particle amplitude $|\tilde{\mathcal{C}}^{(i)}|^2$ of the excited state $|\mathcal{D}_i\rangle$ [Eq. (6)].

Comparing Fig. 6 with Fig. 7, one can further see a first indication that neutron emission at high excitation energy will acquire a well-structured shape due to continuum coupling whereas in the absence of such coupling the neutron emission spectrum would have a flatter shape. This behavior can be illustrated by means of the partial escape width $\tilde{\gamma}_0$ for the decay to the ground state of the residual nucleus [15]. In Fig. 8, the partial escape width $\tilde{\gamma}_0(l_{19/2})$ for the $l_{19/2}$ neutron state in ^{209}Pb to the ground state of ^{208}Pb is shown. It is calculated using an averaging Lorentzian function with $\Delta=0.1$ MeV as in Fig. 1. Comparing Figs. 1 and 8 one can see that the structure in the 17–18 MeV region is more pronounced when the continuum coupling is taken into account.

IV. DISCUSSION

All the results presented in the foregoing section show that the influence of the coupling of the states to the continuum can, generally, not be neglected. It becomes larger with increasing excitation energy. By varying the intensity of the continuum coupling, we have shown how the trapping mechanism takes place in the high-lying part of the spectrum of a nucleus like ^{209}Pb. We have also seen that the single-particle strength distribution is more concentrated when the continuum coupling is included.

The results obtained in the present paper for the $l_{19/2}$ neutron state in ^{209}Pb with realistic wavefunctions coincide with those of more schematic calculations, see, e.g., Ref. [11].

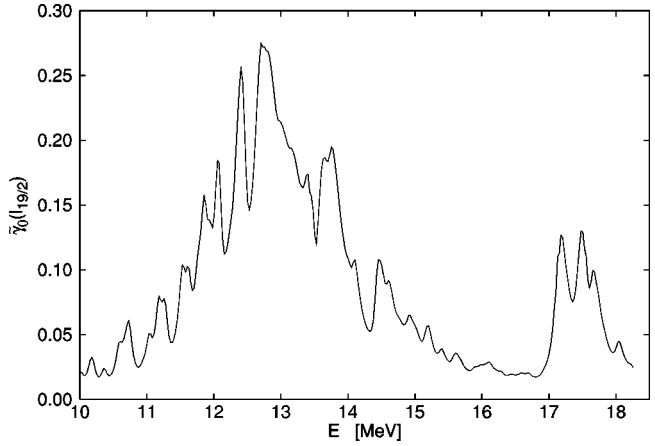

FIG. 8. Partial escape width $\tilde{\gamma}_0(l_{19/2})$ for the decay of the $l_{19/2}$ neutron state in ^{209}Pb to the ^{208}Pb ground state. The partial escape width is calculated using an averaging Lorentzian function with $\Delta = 0.1$ MeV. The unit is in [MeV/MeV].

The interaction is a sum of two parts, the direct (internal) interaction V_{QQ} of the states and their interaction W_{QPQ} via the continuum of decay channels (external interaction). The interplay between these two parts creates states whose collectivity is larger than expected on the basis of calculations without taking the interaction W_{QPQ} via the continuum into account. The collective states are aligned with the decay channels while the remaining states are narrow (trapped). In the calculations for the $l_{19/2}$ state in ^{209}Pb the alignment is demonstrated by means of the spreading of the single-particle strength which is reduced under the influence of the coupling to the continuum. The formation of the aligned states is accompanied by trapping of other states, i.e., by their decoupling from the continuum.

The spreading of the single-particle strength occurs, generally, over a large energy domain. Since the continuum effects depend sensitively on the ratio $\overline{\Gamma}/\overline{D}$ ($\overline{\Gamma}$ average width and $\overline{D}$ average distance of the states), they may be different at the higher-energy part of the spectrum from those at the lower-energy part. Thus the distribution as a whole will differ from that obtained theoretically without taking the coupling via the continuum into account.

In the case studied here, the energy domain ranges from 10 to 19 MeV. The trapping effect is shown to be more important in the energy range around 17.5 MeV than at the energy around 13 MeV. It would be interesting to investigate the influence of the continuum on the structure of high-lying states by performing nucleon-transfer reactions with a particular emphasis on the high energy part of the spectrum.

ACKNOWLEDGMENTS

One of the authors (Ch.S.) has been supported by the Bulgarian Science Foundation (Contract No. Ph.801) and DAAD. He thanks MPI PKS Dresden for hospitality, where the main part of this work has been done. The work has been supported in part by DFG and SMWK Dresden.

[1] S. Galés, Ch. Stoyanov, and A. I. Vdovin, Phys. Rep. **166**, 11 (1988).

[2] S. Fortier, S. Galés, S. M. Austin, W. Benenson, G. M. Crawley, C. Djalali, J. S. Winfield, and G. Yoo, Phys. Rev. C **41**, 2689 (1990).

[3] D. Beaumel, S. Fortier, S. Galés, J. Guillot, H. Langevin-Joliot, H. Laurent, J. M. Maison, J. Vernotte, J. Bordewijk, S. Brandenburg, A. Krasznahorkay, G. M. Crawley, C. P. Massolo, and M. Rentería, Phys. Rev. C **49**, 2444 (1994).

[4] S. Fortier, *Selected Topics in Nuclear Structure*, edited by V. G. Soloviev (JINR, Dubna, 1994), p. 269.

[5] S. Fortier, D. Beaumel, S. Galés, J. Guillot, H. Langevin-Joliot, H. Laurent, J. M. Maison, J. Bordewijk, S. Brandenburg, A. Krasznahorkay, G. M. Crawley, C. P. Massolo, M. Rentería, and A. Khendriche, Phys. Rev. C **52**, 2401 (1995).

[6] Nguyen Van Giai and Ch. Stoyanov, Phys. Lett. B **272**, 178 (1991).

[7] V. G. Soloviev, *Theory of Atomic Nuclei: Quasiparticles and Phonons* (Institute of Physics Publishing, Bristol, 1992).

[8] P. Kleinwächter and I. Rotter, Phys. Rev. C **32**, 1742 (1985); V. V. Sokolov and V. G. Zelevinsky, Nucl. Phys. **A504**, 562 (1989); Ann. Phys. (N.Y.) **216**, 323 (1992); I. Rotter, Rep. Prog. Phys. **54**, 635 (1991); M. Müller, F.-M. Dittes, W. Iskra, and I. Rotter, Phys. Rev. E **52**, 5961 (1995); E. Persson, T. Gorin, and I. Rotter, *ibid.* **54**, 3339 (1996).

[9] V. V. Sokolov, I. Rotter, D. V. Savin, and M. Müller, Phys. Rev. C **56**, 1031 (1997); **56**, 1044 (1997).

[10] E. Persson, T. Gorin, and I. Rotter, Phys. Rev. E **58**, 1334 (1998).

[11] E. Persson and I. Rotter, Phys. Rev. C **59**, 164 (1999).

[12] V. V. Flambaum, A. A. Gribakina, and G. F. Gribakin, Phys. Rev. A **54**, 2066 (1996).

[13] F. Remacle, M. Munster, V. B. Pavlov-Verevkin, and M. Desouter-Lecomte, Phys. Lett. A **145**, 265 (1990); K. Someda, H. Nakamura, and F. H. Mies, Chem. Phys. **187**, 195 (1994); M. Desouter-Lecomte, J. Liévin, and V. Brems, J. Chem. Phys. **103**, 4524 (1995); I. Rotter, *ibid.* **106**, 4810 (1997); U. Peskin, H. Reisler, and W. H. Miller, *ibid.* **106**, 4812 (1997).

[14] E. Persson, K. Pichugin, I. Rotter, and P. Seba, Phys. Rev. E **58**, 8001 (1998).

[15] N. Van Giai, Ch. Stoyanov, V. V. Voronov, and S. Fortier, Phys. Rev. C **53**, 730 (1996).

[16] A. I. Vdovin, V. V. Voronov, V. G. Soloviev, and Ch. Stoyanov, Fiz. Elem. Chastits At. Yadra **16**, 245 (1985) [Sov. J. Part. Nucl. **16**, 105 (1985)].

[17] S. Yoshida and S. Adachi, Z. Phys. A **325**, 441 (1986).

[18] Nguyen Van Giai and Ch. Stoyanov, Phys. Lett. B **252**, 9 (1990).

[19] G. Coló, P. F. Bortignon, Nguyen Van Giai, A. Bracco, and R. A. Broglia, Phys. Lett. B **276**, 279 (1992).

[20] Nguyen Van Giai, Ch. Stoyanov, and V. V. Voronov, in *Selected Topics in Nuclear Structure*, edited by. V. G. Soloviev (JINR, Dubna, 1994), p. 263.
[21] Nguyen Van Giai, Ph. Chomaz, P. F. Bortignon, F. Zardi, and R. A. Broglia, Nucl. Phys. **A482**, 437c (1988).
[22] V. A. Chepurnov, Yad. Fiz. **6**, 955 (1966) [Sov. J. Nucl. Phys. **6**, 696 (1967)].
[23] K. Takeuchi and P. A. Moldauer, Phys. Lett. **28B**, 384 (1969).